Journal of Chromatography A, 1540 (2018) 11–20

Contents lists available at ScienceDirect

Journal of Chromatography A

journal homepage: www.elsevier.com/locate/chroma

Expanding the use of polymeric ionic liquids in headspace solid-phase microextraction: Determination of ultraviolet filters in water samples

María J. Trujillo-Rodríguez, He Nan, Jared L. Anderson*

Department of Chemistry, Iowa State University, Ames, IA 50011, USA

ARTICLE INFO

Article history:
Received 29 November 2017
Received in revised form 23 January 2018
Accepted 23 January 2018
Available online 31 January 2018

Keywords:
Polymeric ionic liquids
Headspace solid-phase microextraction
Gas chromatography–mass spectrometry
Ultraviolet filters
Water analysis

ABSTRACT

Three crosslinked polymeric ionic liquid (PIL) sorbent coatings were used in headspace solid-phase microextraction for the determination of a group of ultraviolet filters. The developed crosslinked PIL-based materials include two polycations and a double confined PIL. The method, in combination with gas chromatography-mass spectrometry, is simple, solvent free, and does not require of any derivatization step. After proper optimization of the methodologies with each developed fiber, the analytical performance was compared with a commercial polyacrylate fiber. A study of the normalized calibration slopes, obtained by dividing the calibration slope of each analyte by the coating volume, revealed that the crosslinked fibers can be used as alternatives to commercial fibers for the determination of the selected group of compounds. In particular, the coating nature of the PIL containing the 1-vinylbenzyl-3-hexadecylimidazolium bis[(trifluoromethyl)sulfonyl]imide IL as monomer and the 1,12-di(3-vinylbenzylimidazolium)dodecane bis[(trifluoromethyl)sulfonyl]imide IL as crosslinker is the most suitable for the extraction of the selected compounds despite their coating volume, being 3.6 times lower than the commercial polyacrylate fiber. For this fiber, wide linear ranges, correlation coefficients higher than 0.990, limits of detection ranging from 2.8 ng L^{-1} to 26 ng L^{-1} and relative standard deviations ranging from 2.5 to 15% were achieved. Finally, all proposed PIL-based fibers were applied towards the analysis of tap water, pool water and lake water, with the majority of the ultraviolet filters being detected and quantified in the last two types of samples.

1. Introduction

Contaminants of emerging concern (CECs) or emerging contaminants include a group of chemicals and other substances widely used since the mid-1990s that pose potential cause of risk in human health. They often have no regulatory standards and have recently been detected in the environmental media [1]. Thus, some of these pollutants are new candidates for future legislation, depending on their eco-toxicity and occurrence, especially in aquatic media [1]. The term CECs includes persistent organic pollutants such as polybrominated diphenyl ethers [2], endocrine disrupting chemicals like some synthetic estrogens or alkylphenols [3], and pharmaceuticals and personal care products (PPCPs) [4]. This last group of compounds comprises a wide variety of prescribed drugs and other compounds used as ingredients in everyday products such as soaps, cosmetics, lotions, fragrances, and sunscreens [4].

Ultraviolet (UV) filters are a group of PPCPs that include both inorganic and organic substances used in everyday products to protect the skin against UV radiation [5]. In particular, organic UV filters like some benzophenones, salicylates, cinnamates and aminobenzoates can be hydrosolubles and can also be absorbed in the skin where they can cause immune system disruption [6]. Furthermore, their extensive use, improper disposal and inefficient treatment of urban wastewater contribute to their presence in the aquatic environment [4]. Thus, the development of monitoring methods for UV filters in waters is of vital importance.

Solid-phase microextraction (SPME) is a powerful extraction and preconcentration technique for the extraction of volatile and semi-volatile compounds [7]. The technique is based on the mass transfer of analytes from the sample to a small volume of sorbent material, normally coated on a solid support. Proper success of SPME is linked to the nature of the sorbent coating of the fiber, among others [7]. However, the commercially-available sorbent materials are not adequate for some applications because they are either not selective, or their extraction efficiency for certain compounds is limited. For that reason, the development of alternative

---

* Corresponding author at: Department of Chemistry, Iowa State University, 1605 Gilman Hall, Ames, IA, 50011, USA.
E-mail address: andersoj@iastate.edu (J.L. Anderson).

https://doi.org/10.1016/j.chroma.2018.01.048
0021-9673/

sorbent materials for SPME is a field of interest in analytical chemistry [8].

Polymeric ionic liquids (PILs) are a group of new materials suitable for their use as SPME sorbent coatings [9]. PILs are polymers generated from the polymerization of an ionic liquid (IL) monomer [10]. Thus, PILs possess most of the unique characteristics of ILs, including low to negligible vapor pressure at room temperature, high chemical and electrochemical stability, and the ability of promote different interactions with analytes. In comparison with ILs, PILs have higher thermal stability and viscosity, making them highly useful materials in high temperature applications [10]. There are different possibilities for the development of PILs, which include polycations, polyanions and polyzwitterions that can be distinguished based on the ionic nature of the cationic, anionic or zwitterionic polymer backbone, respectively [11]. Furthermore, double confined PILs in which both cationic and anionic moieties are co-polymerized have been reported [12]. Other strategies for increasing the stability of the PIL while also increasing their surface area utilizes crosslinked PILs synthesized by the copolymerization of two different ILs: a monocationic IL acting as monomer and a dicationic IL as crosslinker [13].

PILs and crosslinked PILs of the polycationic type have been used in SPME for the determination of different types of CECs, including estrogens [14,15], bisphenol A [14,16], alkylphenols [16,17], and pharmaceuticals [15]. However, there is only one recent study that applied double confined PILs for the determination of UV filters [18]. This work utilized direct immersion (DI)-SPME in combination with high performance liquid chromatography and diode array detection (HPLC-DAD), which resulted in high sorbent coating stability for the analysis of samples possessing high salt content. Other studies also describe DI-SPME-HPLC-UV methods for the determination of UV filters using metal nanoparticles- [19,20] or dodecyltrimethoxysilane-based sorbent coatings [21]. However, the use of gas chromatography-mass spectrometry (GC–MS) allows for increased sensitivity of the methodology, which is required for determining UV filters since they are generally present in aqueous samples at the nanogram per liter level [4]. Some studies reported DI-SPME-GC–MS methods [22,23], or headspace (HS)-SPME-GC–MS methods [24] with commercial fibers for the determination of these compounds. Particularly, the DI-SPME reported methods required the use of derivatization steps, which sometimes are not in accordance with the Green Analytical Chemistry (GAC) [25].

With all of the aforementioned considerations, the main objective of this work was to expand the use of PILs for the determination of a group of CECs such as organic UV filters. With these purposes, different crosslinked PIL-based sorbent coatings have been produced and examined using HS-SPME, including two polycations and a double confined PIL. The extraction efficiency of the PIL-based materials was compared with commercially-available SPME fibers for the determination of this group of analytes. The proposed methodologies, in combination with GC–MS, were also applied for the analysis of real samples, including tap water, pool water and lake water.

2. Experimental

2.1. Chemicals, reagents, materials and samples

The group of determined UV filters includes three salicylates, 2-ethylhexyl salicylate (ES, ≥99.0%), homosalate (HS, pharmaceutical secondary standard) and benzyl-salicylate (BS, ≥99.0%); a benzophenone derivative, benzophenone-3 (BP3, 98.0%); two aminobenzoates, methyl anthranilate (MA, 98%) and ethylhexyl dimethyl PABA or 2-ethylhexyl-4-(dimethylamino)benzoate (EHPABA, 98.0%); and three cinnamates, etocrylene (Eto, 98.0%), 2-ethylhexyl 4-methoxycinnamate (2EHMC, 98.0%) and octocrylene (OCR, ≥98.0%). All UV filters were purchased from Sigma-Aldrich (St. Louis, MO, USA). Table SM-1 of the Supplementary material (SM) shows the structures and some important physicochemical properties of the analytes. Individual stock solutions of the analytes were prepared in acetone (99.0%, Sigma-Aldrich) at 2000 mg L^{-1}. Intermediate solutions containing all analytes were prepared in acetone by dilution of the individual stock solution to 150 mg L^{-1}, 1.00 mg L^{-1}, 0.20 mg L^{-1} or 0.01 mg L^{-1}. Finally, working solutions were prepared by spiking an appropriate amount of an intermediate solution into the sample or ultrapure water containing 25% (w/v) sodium chloride (≥99.5%, purchased from Fisher Scientific, FairLawn, NJ, USA). The organic content of the working solution was 0.1% and 1.6% for optimization and validation experiments, respectively. Ultrapure water (18.2 MΩ cm) was obtained from a Milli-Q water purification system (Millipore, Bedford, MA, USA).

Elastic nitinol wires (external diameter of 127 μm) were acquired from Nitinol Devices & Components (Fremont, CA, USA) and were used as solid supports in the preparation of the SPME fibers. Blank SPME assembly (24 Ga) were provided by Millipore Sigma (Bellefonte, PA, USA).

The commercial polyacrylate (PA, 85 μm of film thickness), polydimethylsiloxane (PDMS, 100 μm of film thickness), carboxen-polydimethylsiloxane (CAR-PDMS, 75 μm of film thickness), and divinylbenzyl/carboxen-polydimethylsiloxane (DVB/CAR-PDMS, 50/30 μm of film thickness) SPME fibers were obtained from Millipore Sigma.

Tap water, pool water and lake water were sampled and collected in Ames (IA, USA). The samples were stored in the dark using plastic bottles at 4 °C before use for a period of time lower than 1 month. Lake water was filtered using a 0.45 μm sterile syringe filter purchased from Corning Incorporated (Corning, Germany). Before analysis, NaCl was added up to a concentration of 25% (w/v).

2.2. Instrumentation

Analyses were carried out using a 7890B GC from Agilent Technologies (Santa Clara, CA, USA) equipped with a 5977A MS detector (single quadrupole) and a HP–5 ms ultra inert capillary column from Agilent Technologies (30 m L × 0.250 mm I.D. × 0.25 μm of film thickness). Ultrapure helium was used as carrier gas at a flow rate of 1 mL min^{-1}. The inlet was operated in *splitless* mode, with an inlet temperature of 290 °C for PA and CAR-PDMS, 270 °C for PDMS and DVB/CAR-PDMS, and 250 °C for the PIL fibers. For the GC oven, the following temperature program was used: initially 100 °C during 1 min, then the temperature was increased at 25 °C min^{-1} up to 290 °C, and held for 5 min. The transfer line from the GC to the MS was kept at 250 °C. The MS was operated in electron ionization (EI) mode at 70 eV, employing gain factor mode and using 230 °C and 150 °C as the source and quadrupole temperatures, respectively. Data was acquired in single ion monitoring (SIM) mode. For the identification of the analytes, three identification points were considered: the retention time, the presence of two of the characteristics ions of each analyte (denoted as quantifier and qualifier ions), and their ratio. The peak area corresponding to the quantifier ion was used for quantitative purposes. The retention time, quantifier and qualifier ions of each UV filters, and the segment program utilized in the MS are shown in Table SM-2 of the SM.

2.3. Procedures

2.3.1. Preparation of the PIL-based SPME fibers

Three different PIL-based SPME fibers were developed in this study, denoted as PIL **1**, PIL **2** and PIL **3**. All fibers were crosslinked PILs, with PIL **1** and PIL **2** as polycations, and PIL **3** as a double con-

Table 1
Composition dimensions and volume of the PIL-based SPME fibers utilized in this study.

PIL fiber	IL monomer	IL crosslinker	Length (cm)	Film thickness[a] (μm)	Volume[b] (μL)
PIL **1**	$[VBC_{16}IM^+][NTf_2^-]$[c]	$[(VBIM)_2C_{12}{}^{2+}]$ $2[NTf_2^-]$[d]	1.3	~23	0.142
PIL **2**	$[VC_{16}IM^+][NTf_2^-]$[e]	$[(VIM)_2C_{12}{}^{2+}]$ $2[NTf_2^-]$[f]	1.3	~81	0.685
PIL **3**	$[VC_{10}IM^+][SS^-]$[g]	$[(VBIM)_2C_{12}{}^{2+}]$ $2[SS^-]$[h]	1.3	~27	0.172

[a] Estimated from Scanning Electron Microscopy (SEM) images.

[b] Calculated using the following expression: $Volume = \pi \left(R^2 - r^2\right) L$, being r the inner radio of the solid support (63.5 μm), R the total radio (63.5 μm + coating film thickness) and L the coating length.

[c] 1-Vinylbenzyl-3-hexadecylimidazolium bis[(trifluoromethyl)sulfonyl]imide.

[d] 1,12-Di(3-vinylbenzylimidazolium)dodecane bis[(trifluoromethyl)sulfonyl]imide.

[e] 1-Vinyl-3-hexadecylimidazolium bis[(trifluoromethyl)sulfonyl]imide.

[f] 1,12-Di(3-vinylimidazolium)dodecane bis[(trifluoromethyl)sulfonyl]imide.

[g] 1-Vinyl-3-decylimidazolium *p*-styrene sulfonate.

[h] 1,12-Di(3-vinylbenzylimidazolium)dodecane *p*-styrene sulfonate.

fined PIL. The preparation of the PIL-based fibers was carried out in three steps: (1) synthesis of the different monomers and crosslinkers, (2) derivatization of the nitinol wires and their assembly in the Millipore Sigma holder, and (3) *on fiber* UV co-polymerization of the IL monomer and IL crosslinker. Table 1 shows the composition (monomer and crosslinker), dimensions and volume of the developed PIL-based fibers.

All IL monomers and crosslinkers were synthesized using previously published methods [26–29]. Procedure SM-1 of the SM briefly describes the synthesis of all ILs. After synthesis, all ILs were characterized using ^{1}H NMR and MS [15–18]. The derivatization of the nitinol wires was also carried out according to published methods [30]. The derivatization consisted of a treatment with hydrogen peroxide to create active hydroxyl moieties (Ti—OH) on the surface of the material, and a subsequent treatment with vinyltrimethoxysilane to create free vinyl groups on the surface of the nitinol. After derivatization, the nitinol wires were glued onto a commercial SPME assembly.

Finally, the co-polymerization was performed by mixing the IL monomer and crosslinker (50%, w/w, respect to the monomer), and the radical initiator (DAROCUR 1173, 3%, w/w, respect to the monomer), following described procedures [13]. The mixture was placed onto the surface of 1.3 cm of the derivatized nitinol and the fibers were exposed to UV irradiation (360 nm) during 2 h using a RPR-100 UV reactor with a spinning carousel purchased from Southern New England Ultraviolet Company (Bradford, CT, USA). The free vinyl groups on the surface of the derivatized nitinol acted as active points to chemically attach the PIL to the solid support. The fibers were then conditioned in the GC injector at 250 °C during 1 h. The film thickness of the coatings was estimated from SEM images.

2.3.2. *Headspace solid-phase microextraction procedure*

10 mL of sample (or aqueous standard solution) containing 0–25% (w/v) NaCl was placed in a 20 mL headspace vial (Restek, Bellefonte, PA, USA). A stir bar (1 cm length × 0.5 cm diameter, from Fisher Scientific) was added and the vial was sealed using a polytetrafluoroethylene (PTFE) crimp cap (Agilent Technologies). The vial was placed on a Corning PC-420D magnetic stirring hotplate (Corning, NY, USA), and the HS-SPME procedure was performed by exposing the fiber to the headspace of the solution, during 20–100 min at 25–100 °C, and fixing the stirring rate to 600 rpm. After extraction, thermal desorption was performed in the GC injector during 2–10 min at 290 °C, 270 °C or 250 °C based on the SPME fiber (see Section 2.2).

Under optimum conditions, HS-SPME is performed using 25% (w/v) of NaCl and 100 °C during 30 min when PIL **3** was used or during 40 min when the remaining fibers were employed. The desorption conditions were 2 min for PA and PIL **2**, and 6 min for PIL **1** and PIL **3** using the desorption temperatures mentioned in Section 2.2.

Analyte *carry over* was evaluated for all fibers. With this purpose, after the analysis of spiked aqueous standard solution samples at optimum conditions, an extra desorption of each fiber in the GC injector was performed for 10 min.

Blank analysis of ultrapure water was carried out once per working day during optimization, between each extraction level during recovery experiments, and between each extraction with real samples.

3. Results and discussion

3.1. *Screening of commercial SPME fibers*

Different commercial SPME fibers were studied for the determination of the UV filters, including PA, PDMS, CAR-PDMS and DVB/CAR-PDMS. Fig. 1 shows the extraction efficiency of all fibers, expressed as chromatographic peak areas for each UV filter. Extractions were performed using 25% (w/v) NaCl at 70 °C, 600 rpm for 20 min, followed by thermal desorption for 6 min. From the results, it is clear that PA, PDMS and DVB/CAR-PDMS are the most suitable fibers for the extraction of the group of selected UV filters while CAR-PDMS poorly extracted the majority of analytes. Analysis of variance (ANOVA) was performed for the three best SPME fibers. The results indicated that no significant differences were observed using any of the fibers tested for ES, HS and MA. Other reported SPME studies for the determination of similar analytes also concluded that the type of commercial fiber have no significant influence in the extraction [22]. Furthermore, PA was more suitable for EHPABA, 2EHMC and OCR. As the sensitivity of these analytes is lower compared to the rest, PA was selected as the optimum commercial fiber. Thus, the extraction performance of the studied PIL-based fibers was compared to the PA fiber.

3.2. *Optimization of the HS-SPME procedure*

The HS-SPME procedure was optimized for PA and the three PIL-based fibers (Table 1) using a factor-by-factor approach. The studied parameters were the NaCl content, the extraction time and temperature, and the desorption time. The other parameters, including sample volume, sampling stirring, the desorption temperature were fixed.

The sample volume was fixed to 10 mL to ensure an adequate preconcentration in the SPME fiber. Furthermore, a high stirring rate (600 rpm) was fixed for all experiments to guarantee an adequate diffusion of the analytes to the headspace. Stir rates higher than 600 rpm were avoided because they created turbulence in the vial, causing the presence of small droplets on the surface of the fiber. Regarding the desorption temperature, a value 10 °C less than

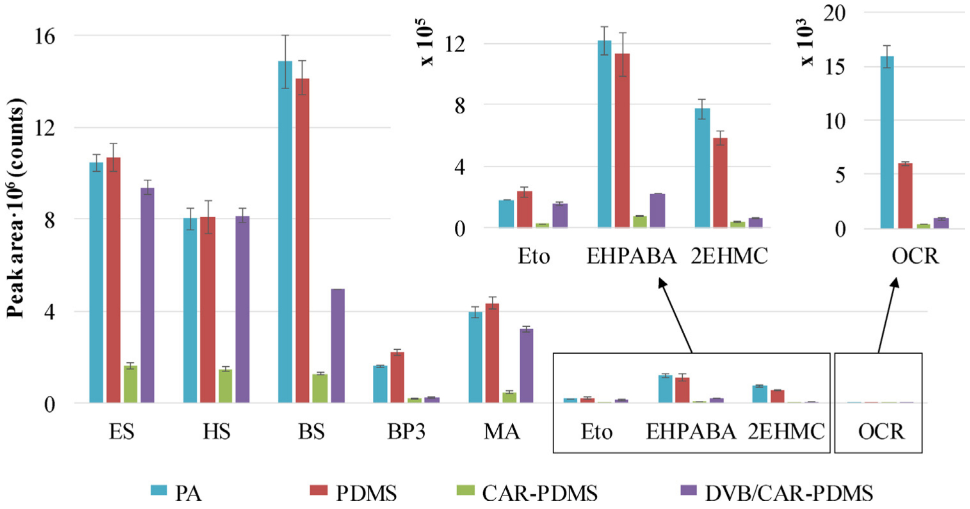

Fig. 1. Extraction efficiency, expressed as chromatographic peak area of UV filters, obtained in the HS-SPME-GC–MS method. Experimental conditions (n = 3): 10 mL of aqueous samples containing UV filters at 100 μg L^{-1}, 25% (w/v) NaCl, HS-SPME extraction (20 min, 70 °C, 600 rpm), desorption (6 min, 290 °C for PA and CAR-PDMS, and 270 °C for PDMS and DVB/CAR-PDMS), and GC–MS.

the maximum admissible temperature of each studied commercial fiber was selected (290 °C or 270 °C depending on the fiber, see Section 2.2). For PIL-based SPME fibers, 250 °C was selected following previously reported methods using similar PILs [13,17]. The objective was to quantitatively desorb the UV filters in the least time possible with no-observed *carry over*, while also preventing decomposition of the coating.

3.2.1. Influence of NaCl content

Previous HS-SPME studies reported that the addition of a salt can improve the extraction efficiency due to the salting out effect [24,31]. This effect is related to the fact that the addition of a salt (as NaCl) to the aqueous sample increases the ionic strength of the aqueous phase, decreasing the solubility of the analytes and increasing their mass transfer to the gas phase. Thus, the influence of the NaCl was evaluated by performing experiments where the NaCl content was varied between 0 and 25% (w/v). Fig. SM-1 of the SM shows the results for all fibers. Extractions were performed at 70 °C, 600 rpm for 20 min, followed by thermal desorption for 6 min. As expected, the highest extraction efficiencies were achieved using 25% (w/v) NaCl with any of the fibers tested. Therefore, 25% (w/v) NaCl was selected as optimum for all fibers. In addition, the results demonstrated that the enhancement in extraction efficiency is sharper for PIL-based fibers than for the PA fiber. The exception was PIL **3**, for which EHPABA and 2EHMC achieved the maximum extraction efficiency using 15% (w/v) NaCl.

3.2.2. Influence of extraction temperature

The extraction temperature is a key factor in HS-SPME. On one hand, an increase in the extraction temperature enhances the mass transfer of analytes from the aqueous sample to the headspace. However, the overall partition coefficient of analytes between the sample and the fiber also decreases due to the extraction process generally being exothermic [7]. For that reason, the influence of extraction temperature in the extraction efficiency of UV filters was studied for all fibers by performing experiments with temperatures between 25 and 100 °C using 25% (w/v) NaCl, 600 rpm for 20 min, followed by thermal desorption for 6 min. Fig. 2 shows the obtained results for PIL **1** as a representative example, while the results for the remaining fibers are presented in Fig. SM-2 of the SM.

The behavior of both PA and PIL-based fibers was similar. In general, the extraction efficiency increased with temperature up to 70 °C for two of the salicylates (ES and HS) due to an increase in the mass transfer of the analytes to the headspace. However, increasing

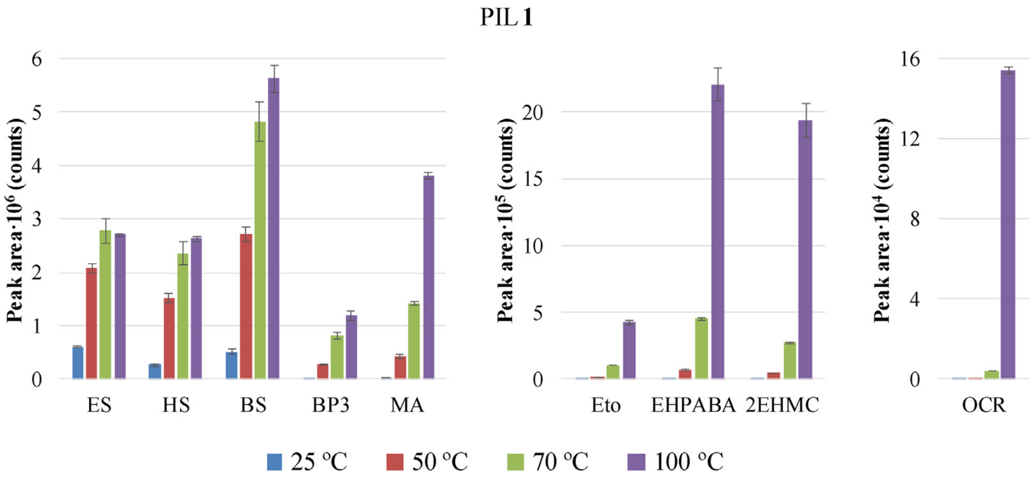

Fig. 2. Influence of the extraction temperature in the HS-SPME-GC–MS method obtained for PIL **1** as a representative example of all the studied fibers. Experimental conditions (n = 3): 10 mL of aqueous samples containing UV filters at 100 μg L^{-1}, 25% (w/v) NaCl, HS-SPME extraction (20 min, 25–100 °C, 600 rpm), desorption (6 min, 250 °C), and GC–MS.

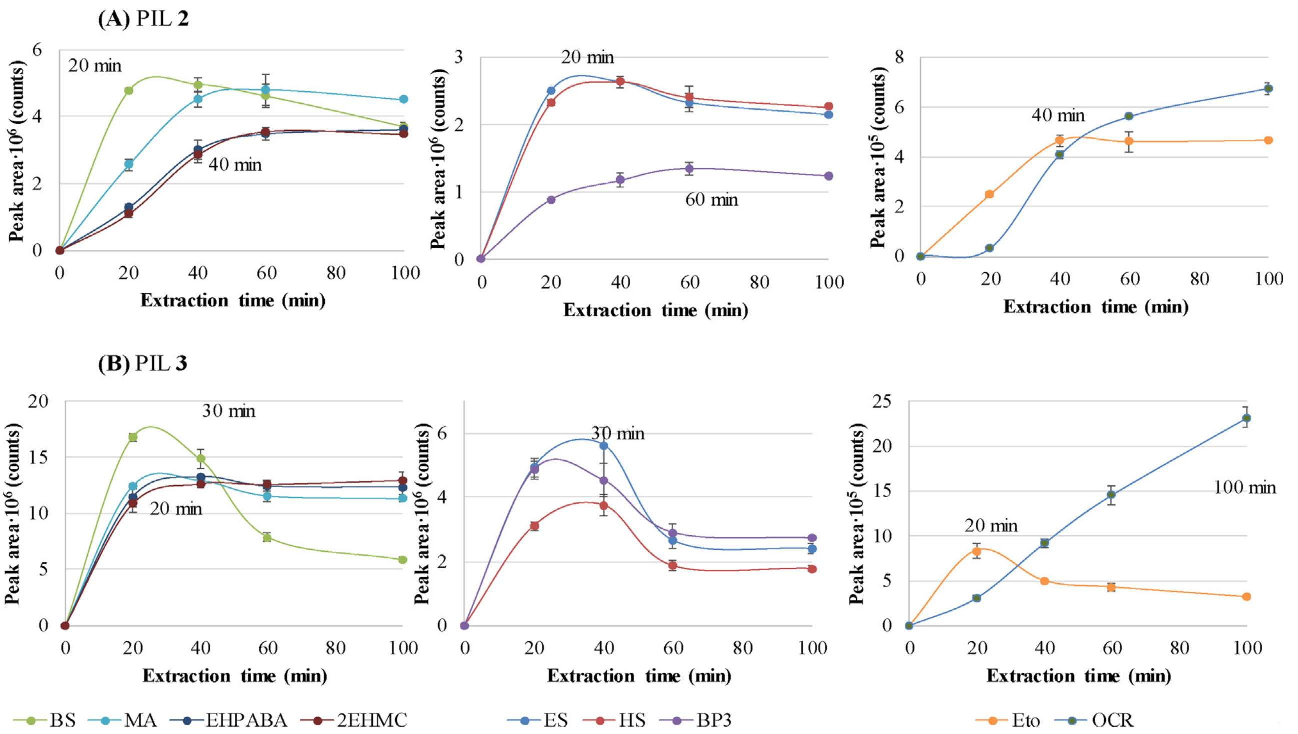

Fig. 3. Extraction time profiles obtained for the HS-SPME-GC–MS method using **(A)** PIL **2**, and **(B)** PIL **3** as representative fibers. Experimental conditions (n = 3): 10 mL of aqueous samples containing UV filters at 100 μg L^{-1}, 25% (w/v) NaCl, HS-SPME extraction (20–100 min, 100 °C, 600 rpm), desorption (6 min, 290 °C), and GC–MS.

the extraction temperature from 70 °C to 100 °C caused a decrease in the extraction efficiency for those analytes, probably due to these analytes preferring to reside in the gas phase rather in the sorbent coating. This effect was observed for both analytes when PA was used, and for ES using PIL **1** and PIL **3**. In the remaining cases involving the studied UV filters and all SPME fibers, heating the extraction vial always have a positive effect on the extraction efficiency. The increase of the extraction efficiency is more pronounced from 70 °C to 100 °C, and for the most hydrophobic compounds (EHPABA, 2EHMC and OCR). With all these considerations, 100 °C was selected as the optimum extraction temperature for all tested fibers.

3.2.3. Influence of extraction time

The extraction time is another important factor to consider in SPME. As SPME is a multiphase equilibration process, the maximum extraction efficiency is achieved working under equilibrium conditions. However, for analytes with low Henry's law constants, the time needed to reach equilibrium is higher. In these cases, extraction times lower than the equilibrium time are selected if at those conditions the sensitivity of the method is adequate. Considering the importance of this parameter, the extraction time was studied for PA and all PIL-based fibers in the range between 20 and 100 min. Fig. 3 shows the extraction time profiles obtained for UV filters using PIL **2** and PIL **3** as representative examples. The results obtained for the remaining fibers are presented in Fig. SM-3 of the SM.

Different trends were observed for the analytes. From Fig. 3, it is clear that for the majority of the analytes, and especially the most hydrophobic, the extraction efficiency increases up to and reaches a maximum and then levels off. However, for the salicylates (ES, HS and BS), the extraction efficiency increases up to a maximum and then slightly decreases, probably because these compounds suffer desorption from the fiber into the HS at longer extraction times. In these cases, the continued stirring can caused an increase in the vial temperature at longer extraction times, causing the desorption processes.

Regarding the commercial PA fiber, 20 min was the equilibrium time for ES, HS, and BS, while longer equilibration times (between 20 and 40 min) were required for BP3, MA, EHPABA, 2EHMC, and Eto, and 60 min required for OCR. For PIL **1**, 40 min was the equilibration time for the majority of analytes, with the exception of BS and OCR for which 20 min and 60 min, respectively, were needed to achieve equilibrum. When PIL **2** was used (Fig. 3), 20 min was required to reach equilibrium for ES, HS and BS, 60 min for BP3, 50 min for OCR, and 40 min for the remaining analytes. Considering PIL **3** (Fig. 3), 20 min was required for MA, EHPABA, 2EHMC and Eto, and 30 min for ES, HS, BS and BP3. Furthermore, OCR did not achieved equilibration in the time range studied when PIL **3** was tested. With all these considerations, 40 min was selected as the optimum extraction time for PA, PIL **1** and PIL **2**, and 30 min for PIL **3**.

3.2.4. Influence of desorption time

An adequate desorption time in the GC inlet is required to quantitatively desorb all analytes and to avoid the *carry over* effect. Thus, the influence of the desorption time was studied in the range between 2 and 10 min. Fig. SM-4 of the SM shows the desorption time profiles for all fibers. The results indicated that 2 min was adequate for the quantitative desorption of analytes using PA and PIL **2**, while 6 min was required for PIL **1** and PIL **3**. No significant *carry over* was observed under these conditions.

3.3. Analytical performance of the developed HS-SPME methods

After the proper optimization of the HS-SPME methods using different fibers, they were validated by the development of external calibration curves of UV filters. The analytical performance of the methods was evaluated in terms of the linearity ranges, correlation coefficient (R), sensitivities, limits of detection (LODs), and limit of

Table 2
Analytical figures of merit obtained for UV filters when HS-SPME-GC–MS extractions are performed using different SPME fibers.

Analyte	Working range (ng L^{-1})				(Calibration slope ± SD[a]) 10^{-3}				LOD[b] (ng L^{-1})			
	PA	PIL 1	PIL 2	PIL 3	PA	PIL 1	PIL 2	PIL 3	PA	PIL 1	PIL 2	PIL 3
ES	10–1200	10–1200	20–1200	50–510	15.7 ± 0.7	8.1 ± 0.2	16.8 ± 0.4	0.52 ± 0.01	5.7	3.4	5.2	28
HS	10–1200	40–1200	40–1200	100–3000	16.7 ± 0.6	9.5 ± 0.2	18.4 ± 0.3	0.61 ± 0.01	1.2	13	12	33
BS	1–50	1–50	10–60	200–5000	23 ± 7	2.8 ± 0.9	8.9 ± 2	0.50 ± 0.02	1.1	7.7	6.9	55
BP3	10–1000	50–1200	40–1200	50–5000	1.1 ± 0.1	0.64 ± 0.02	0.99 ± 0.02	0.075 ± 0.003	3.3	17	12	12
MA	10–1000	10–1200	40–1200	100–5000	30 ± 1	20.5 ± 0.4	30.1 ± 0.5	1.8 ± 0.03	5.0	2.8	4.0	27
Eto	10–1000	50–1200	30–1000	200–6000	0.30 ± 0.01	0.29 ± 0.01	0.42 ± 0.01	0.029 ± 0.001	41	21	14	47
EHPABA	10–900	10–1300	50–1300	50–6000	21 ± 1	13.1 ± 0.3	16.0 ± 0.4	1.67 ± 0.04	4.2	2.5	5.0	17
2EHMC	10–600	20–1000	40–1200	50–6000	20 ± 1	13.2 ± 0.5	16.6 ± 0.6	2.6 ± 0.1	4.5	5.4	13	9.2
OCR	200–800	90–1000	150–1200	100–6000	0.43 ± 0.05	0.28 ± 0.01	0.19 ± 0.01	0.054 ± 0.002	70	26	46	29

[a] Standard deviation of the slope.
[b] Limit of detection, calculated as the concentration corresponding to 3 times the signal-to-noise ratio.

Table 3
Relative standard deviation (RSD) and relative recovery (RR) obtained for UV filters when HS-SPME-GC–MS extractions are performed using different SPME fibers.

Analytes	Spiked level 1								Spiked level 2							
	PA[a]		PIL 1[b]		PIL 2[b]		PIL 3[c]		PA[d]		PIL 1[e]		PIL 2[e]		PIL 3[f]	
	RSD (%)	RR (%)	RSD (%)	RR (%)	RSD (%)	RR (%)	RSD (%)	RR (%)	RSD (%)	RR (%)	RSD (%)	RR (%)	RSD (%)	RR (%)	RSD (%)	RR (%)
ES	11	91.3	10	82.4	4.6	101	4.5	108	5.2	106	3.3	110	7.3	102	12	96.7
HS	4.3	90.0	5.1	82.9	4.2	91.6	2.9	92.1	8.3	99.3	6.6	114	6.6	99.5	11	94.9
BS	15	120	8.0	82.2	8.7	111	12	91.9	1.5	80.7	9.6	79.7	12	95.2	13	102
BP3	8.4	94.6	3.4	103	10	81.1	5.5	106	1.8	80.9	10	75.3	4.4	103	4.0	118
MA	6.7	109	3.9	82.1	2.0	102	1.3	113	13	77.3	3.9	94.3	12	87.2	9.8	109
Eto	6.1	93.4	2.5	78.6	11	86.9	8.3	96.2	5.0	96.1	14	90.1	8.2	108	6.4	100
EHPABA	6.5	103	11	84.1	6.1	107	2.7	113	12	84.5	9.5	86.8	11	87.2	3.2	113
2EHMC	10	105	7.2	75.6	9.7	101	6.8	108	13	79.8	6.9	85.7	8.9	85.8	5.1	120
OCR	17	103	15	113	15	119	10	110	16	85.1	17	63.5	4.8	106	13	116

[a] 8 ng L^{-1} for BS, 160 ng L^{-1} for the rest of analytes.
[b] 8 ng L^{-1} for BS, 200 ng L^{-1} for the rest of analytes.
[c] 0.8 μg L^{-1} for BS, 1 μg L^{-1} for the rest of analytes.
[d] 30 ng L^{-1} for BS, 300 ng L^{-1} for EHPABA, and 600 ng L^{-1} for the rest of analytes.
[e] 25 ng L^{-1} for BS, 500 ng L^{-1} for the rest of analytes.
[f] 2.5 μg L^{-1} for all analytes.

quantifications (LOQs). All these parameters are included in Tables SM-3-6 of the SM.

The calibration curves presented wide linear ranges for all UV filters using all fibers. Table 2 shows the working ranges for each UV filter and each SPME fiber. The R values ranged from 0.990 to 0.995 when PA was utilized, from 0.990 to 0.999 for PIL **1** and PIL **2**, and from 0.994 to 0.999 for PIL **3**.

Table 2 also includes the sensitivity of the method using each SPME fiber, expressed as the calibration slopes. The values ranged from $(0.30 \pm 0.01)\cdot10^{-3}$ to $(30 \pm 1)\cdot10^{-3}$ when PA was used, from $(0.28 \pm 0.01)\cdot10^{-3}$ to $(20.5 \pm 0.4)\cdot10^{-3}$ when PIL **1** was employed, from $(0.19 \pm 0.01)\cdot10^{-3}$ to $(30.1 \pm 0.5)\cdot10^{-3}$ using PIL **2**, and from $(0.029 \pm 0.001)\cdot10^{-3}$ to $(2.6 \pm 0.1)\cdot10^{-3}$ using PIL **3**. It is important to highlight that the calibration slopes obtained for PIL **1** and PIL **2** are comparable to those obtained for the commercial PA fiber. Thus, PA presents similar sensitivity to PIL **1** in the case of Eto, and to PIL **2** for ES, HS, BP3 and MA. Furthermore, the sensitivity of PIL **2** is 1.5 times higher than the sensitivity of PA for the extraction of Eto (Table 2).

The LODs and LOQs were determined as the concentration corresponding to three or ten times the signal-to-noise ratio of blank samples, respectively. Table 2 also includes the LOD values that were verified by performing extractions at the obtained LOD levels. The LODs ranged from 1.1 ng L^{-1} to 70 ng L^{-1} using PA, from 2.8 ng L^{-1} to 26 ng L^{-1} using PIL **1**, between 4.0 ng L^{-1} and 46 ng L^{-1} for PIL **2**, and between 9.2 ng L^{-1} to 47 ng L^{-1} using PIL **3**. It is important to again highlight that results obtained for the PIL-based fibers, especially for PIL **1** and PIL **2**, are comparable with those obtained for the commercial PA fiber.

The results regarding the reproducibility and the accuracy of the method with each fiber are presented in Table 3. The reproducibility was estimated as the relative standard deviation (RSD) obtained after performing intra-day experiments ($n = 3$) at two spiked levels of UV filters. For the lower spiked level, the RSD ranged from 4.3 to 17% for PA, from 2.5 to 15% for PIL **1**, from 4.2 to 15% for PIL **2**, and from 1.3 to 10% for PIL **3**. The accuracy of the methodologies was estimated as relative recovery (RR). The RRs were calculated as the ratio of the predicted concentration obtained using the calibration curves of the entire method and the spiked concentration for each UV filter. The same spiked levels used in the reproducibility studies were used for recovery. For the low spiked level, the RRs ranged from 90.0 to 120% using PA, from 78.6 to 113% for PIL **1**, from 81.1 to 119% for PIL **2**, and from 91.9 to 113% for PIL **3**.

Finally, the developed methods were compared with other methodologies reported in the literature that use GC–MS for the determination of UV filters (Table SM-7 of the SM). There are few methods that utilize SPME-GC–MS [22–24]. These methods reported similar analytical performance than the current methodology in terms of linearity range, LODs, reproducibility and relative recovery. However, the reported DI-SPME-GC–MS methods require derivatization of the analytes [22,23]. Some methods integrate the derivatization with other analytical processes which definitely aids in the simplification of the methodology [23]. Other studies used microextraction techniques such as dispersive liquid–liquid microextraction (DLLME) [32] or ultrasound-assisted emulsification microextraction (UAEME) [33]. SPME is as simple as these techniques, but it is important to highlight the reusability of the extraction material (the PIL-based SPME fiber) in comparison with liquid-phase microextraction procedures. Thus, the proposed

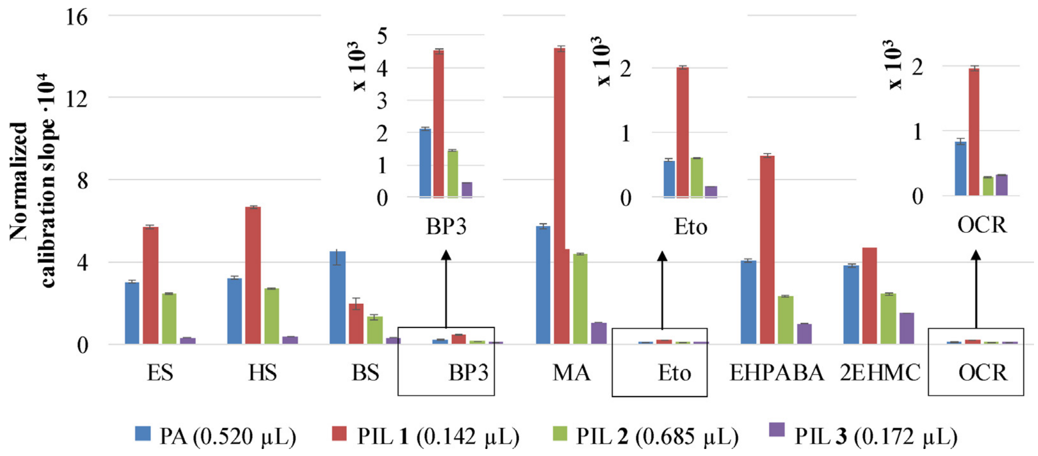

Fig. 4. Normalized calibration slopes (ratio of the calibration slope of the HS-SPME-GC–MS and the volume coating of the SPME fiber) obtained for UV filters using different SPME fibers.

methods using PIL-based SPME fibers represent a faster, simpler and environmentally friendlier alternative method for the determination of UV filters.

3.4. Comparison of the extraction efficiency of the fibers under optimum HS-SPME conditions

A comparison of the analytical figures of merit previously discussed is Section 3.3 serves to demonstrate the suitability of the developed PIL-based fibers for the determination of the selected group of UV filters. The results in Tables 2 and 3 also confirms that the extraction performance of the fibers is comparable to the commercial PA fiber. However, the established comparison takes into consideration all the factors affecting the HS-SPME extraction, including the nature of the sorbent coating and the volume of coating (that is proportional to the length and film thickness of the coating). Previously published works reported the use of normalized calibration slopes as a tool to compare the extraction efficiency of the fibers by only considering their nature [17,31,34]. In those reported studies, all coatings had the same length (1 cm). Thus, the normalized calibration slopes were calculated by dividing each calibration slope by the film coating. In this particular case, the developed PIL-based fibers have a different length and film thickness (see Table 1) than the commercial PA fiber. For that reason, normalization has been carried out by dividing each calibration slope by their coating volume. The obtained results for all tested fibers, including PIL-based fibers and PA, are presented in Fig. 4. PIL **2** has a similar coating volume than the commercial PA fiber (0.685 µL for PIL **2** *versus* 0.520 µL for PA) while the other PIL-based fibers (PIL **1** and PIL **3**) have a significantly low volume (Table 1). It is important to highlight that these results only serve as an estimation to compare the extraction efficiency of all studied fibers, while the best approach to study the influence of the coating nature is by comparing the partition coefficient that analytes undergo between the aqueous solution to each SPME fiber.

From Fig. 4, it is clear that the coating nature of PIL **1** is the most suitable for the extraction of the selected group of compounds, with the exception of BS for which the PA coating is more beneficial. Thus, normalized calibration slopes for PIL **1** were between 1.9 and 3.5 times higher than for PA, excluding BS. The results also demonstrated that PIL **1** is especially beneficial for the extraction of Eto. Furthermore, the normalized calibration slopes for PIL **2** and PA are comparable, which indicates that the affinity of UV filters for those polymeric materials is similar. The obtained results demonstrate that PIL **1** and PIL **2** can be used as alternatives to commercial fibers for the determination of the selected group of UV filters.

The lowest normalized calibration slopes were achieved for PIL **3**. These results are also in accordance with the obtained LODs of the developed methods (Table 2). PIL **3** had been recently used in a DI-SPME method in combination with high performance liquid chromatography with diode array detection (HPLC-DAD) [18]. The presence of the polymerizable *p*-styrene sulfonate anion in the structure of both monomer and crosslinker improved the stability of the fiber when samples possessing high salt content were extracted by DI-SPME. In HS-SPME, the fiber is exposed to the headspace created in the extraction vial and, consequently, the salinity of the sample does not affect the stability of the fiber. However, in this application, the presence of the *p*-styrene sulfonate anion can promote a different polymer architecture with respect to the polycationic coatings PIL **1** and PIL **2**, which can change the morphology and/or surface area of the final polymer, affecting in the extraction efficiency. Furthermore, the presence of long alkyl chains in the structure of the cation of the IL monomers of PIL **1** and PIL **2** explains the improvement in the extraction efficiency with respect to PIL **3**. On the other hand, if PIL **1** and PIL **2** are only compared, the presence of benzyl groups in both the monomer and crosslinker of PIL **1** can promote π-π interactions with the aromatic rings of UV filters, explaining the increase in the normalized calibration slopes. This behavior was previously observed with similar PIL-based fibers for the extraction of other types of aromatic compounds [17].

3.5. Analysis of real samples

To test the applicability of the developed PIL-based fibers, different water samples were analyzed, including tap water, pool water and lake water.

None of the studied UV filters were detected in tap water. Thus, the possible matrix effect that this sample could exert in the developed methodologies was studied through the analysis of spiked tap water. Fig. 5 shows a representative chromatogram obtained after the analysis of spiked tap water samples using PIL **1**, being the most suitable fiber for the determination of the selected group of UV filters. The matrix effect was evaluated in terms of reproducibility and RR, and using the spiked level 1 used in Table 3 for extractions performed using aqueous standard solutions. For spiked tap water samples, the RSDs were acceptable, ranging from 3.5 to 15% using PA, 5.5–12% when PIL **1** was employed, 1.6–13% using PIL **2**, and 2.6–8.3% when PIL **3** was used. The RRs ranged from 73.3 to 109% using PA, from 72.0 to 118% using PIL **1**, from 72.7 to 122% using PIL **2**, and from 72.5 to 111% when PIL **3** was used. Table SM-8 shows the obtained values for each UV filter. These results are compara-

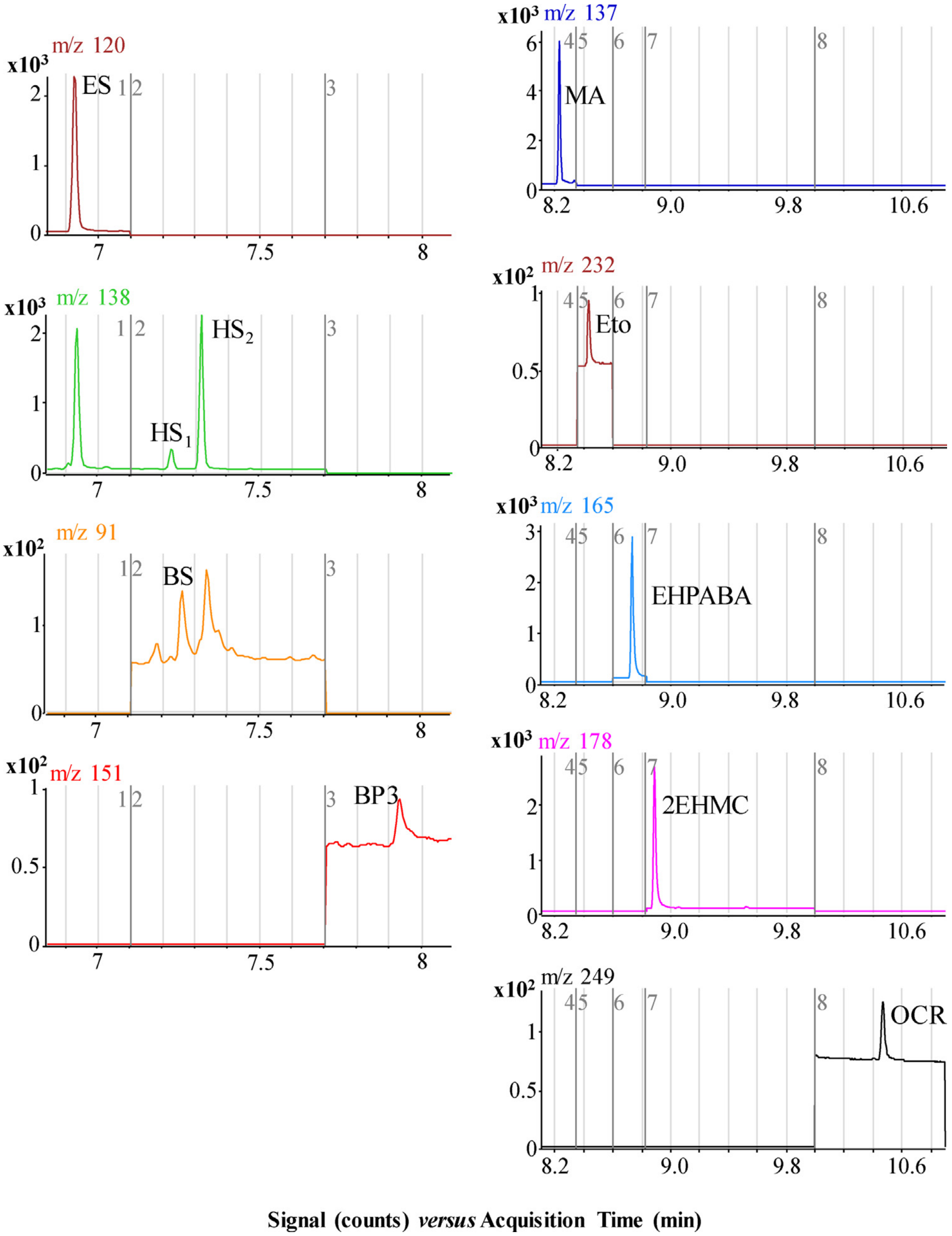

Fig. 5. Representative chromatogram obtained after the analysis of spiked tap water using PIL **1**.

ble with those obtained using aqueous standard solutions (Table 3). Thus, it can be concluded that there is no significant matrix effect for tap water.

Regarding the analysis of pool water and lake water, Table 4 shows the obtained results obtained for PA, PIL **1** and PIL **2**. BS, BP3, Eto and EHPABA were not detected in any of the analyzed samples. The remaining analytes were present in the samples at concentrations close to the LOQ of the methods, which implies that matrix matched calibrations and/or standard addition calibrations are required in order to confirm the absence of matrix effect in pool and river water. However, the results obtained between fibers are comparable, and these analytes were previously determined in other pool and river waters via HS-SPME-GC–MS using the PA fiber [24]. It is important to mention that some organic UV filters have been identified as potential endocrine disrupting compounds [6]. Thereby, toxicological studies concluded that cinnamate derivatives such as 2EHMC and OCR, detected in the analyzed samples, can cause disrupting effects towards estrogen receptors [35] and thyroid hormone receptors [36], among others. Thus, the monitoring of these compounds in water is of vital importance.

4. Conclusions

Three different crosslinked PIL sorbent coatings were successfully applied in a HS-SPME-GC–MS method for the determination of organic UV filters, including three salicylates, a benzophenone derivative, two aminobenzoates, and three cinnamates.

After proper optimization of the methodology with each fiber, the extraction performance of the developed PIL-based SPME fibers was extensively compared with the commercial PA fiber, which was the most suitable fiber for the extraction of the group of selected UV filters. The results indicated that the analytical performance of the PIL fibers and PA were comparable in terms of linearity range, correlation coefficients, LOD, reproducibility and RR, especially for PIL **1** and PIL **2**. A detailed comparison between the different sorbent coatings was established by the estimation of the normalized

Table 4
Analysis of pool water and lake water using the HS-SPME-GC–MS methods with different SPME fibers.

Analyte	Found concentration (error[a]) (ng L^{-1})					
	Pool water			Lake water		
	PA	PIL 1	PIL 2	PA	PIL 1	PIL 2
ES	31 (2)	34 (15)	18 (7)	23 (9)	34 (19)	31 (18)
HS	32 (1)	>LOD [b]	17 (8)	42 (17)	>LOD	27 (13)
MA	11 (3)	12 (3)	>LOD	7 (2)	12 (5)	>LOD
2EHMC	20 (3)	81 (12)	>LOD	31 (5)	35 (12)	32 (4)
OCR	>LOD	>LOD	>LOD	n.d.[c]	n.d.	n.d.

* BS, BP3, Eto and EHPABA were not detected in any of the analyzed samples.
[a] Error associated to the determination.
[b] Detected but non-quantified.
[c] Not detected.

calibration slopes, indicating that the nature of the PIL **1** sorbent coating is the most suitable for the extraction of the selected group of UV filters. Normalized calibration slopes between 1.9 and 3.5 times higher than for PA were obtained, with the exception of BS. These results were explained due to the presence of benzyl groups in both the monomer and crosslinker of PIL **1**, which can promote π-π interactions with the aromatic rings of UV filters. Finally, the proposed methods were applied towards the analysis of tap water, pool water and lake water, with ES, HS, MA, and 2EHMC being determined in pool and lake water.

Acknowledgement

JLA acknowledges funding from Chemical Measurement and Imaging Program at the National Science Foundation (Grant number CHE-1709372).

Appendix A. Supplementary data

Supplementary data associated with this article can be found, in the online version, at https://doi.org/10.1016/j.chroma.2018.01.048.

References

[1] United States Environmental Protection Agency (EPA), Contaminants of Emerging Concern Including Pharmaceuticals and Personal Care Products, 2016 (Accessed 28 November 2017) https://www.epa.gov/wqc/contaminants-emerging-concern-including-pharmaceuticals-and-personal-care-products/.
[2] S. Król, B. Zabiegała, J. Namieśnik, PBDEs in environmental samples: sampling and analysis, Talanta 93 (2012) 1–17.
[3] T.F.T. Omar, A. Ahmad, A.Z. Aris, F.M. Yusoff, Endocrine disrupting compounds (EDCs) in environmental matrices: review of analytical strategies for pharmaceuticals, estrogenic hormones, and alkylphenol compounds, Trends Anal. Chem. 85 (2016) 241–259.
[4] D. Montes-Grajales, M. Fennix-Agudelo, W. Miranda-Castro, Occurrence of personal care products as emerging chemicals of concern in water resources: a review, Sci. Total Environ. 595 (2017) 601–614.
[5] M. Lores, M. Llompart, G. Alvarez-Rivera, E. Guerra, M. Vila, M. Celeiro, J.P. Lamas, C. Garcia-Jares, Positive lists of cosmetic ingredients: analytical methodology for regulatory and safety controls—a review, Anal. Chim. Acta 915 (2016) 1–26.
[6] J. Wang, L. Pan, S. Wu, L. Lu, Y. Xu, Y. Zhu, M. Guo, S. Zhuang, Recent advances on endocrine disrupting effects of UV filters, Int. J. Environ. Res. Public Health 13 (2016) 782.
[7] J. Pawliszyn, Handbook of Solid Phase Microextraction, Elsevier, Waltham, MA USA, 2012.
[8] E.A. Souza-Silva, R. Jiang, A. Rodríguez-Lafuente, E. Gionfriddo, J. Pawliszyn, A critical review of the state of the art of solid-phase microextraction of complex matrices I. Environmental analysis, Trends Anal. Chem. 71 (2015) 224–235.
[9] K.D. Clark, M.N. Emaus, M. Varona, A.N. Bowers, J.L. Anderson, Ionic liquids: solvents and sorbents in sample preparation, J. Sep. Sci. 41 (2017) 209–235.
[10] W. Qian, J. Texter, F. Yan, Frontiers in poly(ionic liquid)s: syntheses and applications, Chem. Soc. Rev. 46 (2017) 1124–1159.
[11] D. Mecerreyes, Polymeric ionic liquids: broadening the properties and applications of polyelectrolytes, Prog. Polym. Sci. 36 (2011) 1629–1648.
[12] J. Feng, M. Sun, L. Xu, S. Wang, X. Liu, S. Jiang, Novel double-confined polymeric ionic liquids as sorbents for solid-phase microextraction with enhanced stability and durability in high-ionic-strength solution, J. Chromatogr. A 1268 (2012) 16–21.
[13] T.D. Ho, H. Yu, W.T.S. Cole, J.L. Anderson, Ultraviolet photoinitiated on-fiber copolymerization of ionic liquid sorbent coatings for headspace and direct immersion solid-phase microextraction, Anal. Chem. 84 (2012) 9520–9528.
[14] M. Pei, Z. Zhang, X. Huang, Y. Wu, Fabrication of a polymeric ionic liquid-based adsorbent for multiple monolithic fiber solid-phase microextraction of endocrine disrupting chemicals in complicated samples, Talanta 165 (2017) 152–160.
[15] H. Yu, J. Merib, J.L. Anderson, Crosslinked polymeric ionic liquids as solid-phase microextraction sorbent coatings for high performance liquid chromatography, J. Chromatogr. A 1438 (2016) 10–21.
[16] I. Pacheco-Fernández, A. Najafi, V. Pino, J.L. Anderson, J.H. Ayala, A.M. Afonso, Utilization of highly robust and selective crosslinked polymeric ionic liquid-based sorbent coatings in direct-immersion solid-phase microextraction and high-performance liquid chromatography for determining polar organic pollutants in waters, Talanta 158 (2016) 125–133.
[17] M. Cordero-Vaca, M.J. Trujillo-Rodríguez, C. Zhang, V. Pino, J.L. Anderson, A.M. Afonso, Automated direct-immersion solid-phase microextraction using crosslinked polymeric ionic liquid sorbent coatings for the determination of water pollutants by gas chromatography, Anal. Bioanal. Chem. 407 (2015) 4615–4627.
[18] J. An, J.L. Anderson, Determination of Uv filters in high ionic strength sample solutions using matrix-compatible coatings for solid-phase microextraction, Talanta (2018), http://dx.doi.org/10.1016/j.talanta.2018.01.052, in press.
[19] L. Li, R. Guo, Y. Li, M. Guo, X. Wang, X. Du, In situ growth and phenyl functionalization of titania nanoparticles coating for solid-phase microextraction of ultraviolet filters in environmental water samples followed by high performance liquid chromatography–UV detection, Anal. Chim. Acta 867 (2015) 38–46.
[20] M. Ma, H. Wang, Q. Zhen, M. Zhang, X. Du, Development of nitrogen-enriched carbonaceous material coated titania nanotubes array as a fiber coating for solid-phase microextraction of ultraviolet filters in environmental water, Talanta 167 (2017) 118–125.
[21] J. Li, L. Ma, M. Tang, L. Xu, C_{12}-Ag wire as solid-phase microextraction fiber for determination of benzophenone ultraviolet filters in river water, J. Chromatogr. A 1298 (2013) 1–8.
[22] M. Vila, M. Celeiro, J.P. Lamas, C. Garcia-Jares, T. Dagnac, M. Llompart, Simultaneous *in-vial* acetylation solid-phase microextraction followed by gas chromatography tandem mass spectrometry for the analysis of multiclass organic UV filters in water, J. Hazard. Mater. 323 (2017) 45–55.
[23] N. Negreira, I. Rodríguez, M. Ramil, E. Rubí, R. Cela, Sensitive determination of salicylate and benzophenone type UV filters in water samples using solid-phase microextraction, derivatization and gas chromatography tandem mass spectrometry, Anal. Chim. Acta 638 (2009) 36–44.
[24] M. Vila, M. Celeiro, J.P. Lamas, T. Dagnac, M. Llompart, C. Garcia-Jares, Determination of fourteen UV filters in bathing water by headspace solid-phase microextraction and gas chromatography-tandem mass spectrometry, Anal. Methods 8 (2016) 7069–7079.
[25] A. Gałuszka, Z. Migaszewski, J. Namieśnik, The 12 principles of green analytical chemistry and the significance mnemonic of green analytical practices, Trends Anal. Chem. 50 (2013) 78–84.
[26] J.L. Anderson, D.W. Armstrong, Immobilized ionic liquids as high-selectivity/high-temperature/high-stability gas chromatography stationary phases, Anal. Chem. 77 (2005), 6453–6452.
[27] J.L. Anderson, R. Ding, A. Ellern, D.W. Armstrong, Structure and Properties of high stability geminal dicationic ionic liquids, J. Am. Chem. Soc. 127 (2005) 593–604.
[28] Q.Q. Baltazar, J. Chandawalla, K. Sawyer, J.L. Anderson, Interfacial and micellar properties of imidazolium-based monocationic and dicationic ionic liquids, Colloid Surf. A-Physicochem. Eng. Asp. 302 (2007) 150–156.
[29] Y. Meng, J.L. Anderson, Tuning the selectivity of polymeric ionic liquid sorbent coatings for the extraction of polycyclic aromatic hydrocarbon using solid-phase microextraction, J. Chromatogr. A 1217 (2010) 6143–6152.

[30] T.D. Ho, B.R. Toledo, L.W. Hantao, J.L. Anderson, Chemical immobilization of crosslinked polymeric ionic liquids on nitinol wires produces highly robust sorbent coatings for solid-phase microextraction, Anal. Chim. Acta 843 (2014) 18–26.

[31] M.J. Trujillo-Rodríguez, H. Yu, W.T.S. Cole, T.D. Ho, V. Pino, J.L. Anderson, A.M. Afonso, Polymeric ionic liquid coatings versus commercial solid-phase microextraction coatings for the determination of volatile compounds in cheeses, Talanta 121 (2014) 153–162.

[32] J.L. Benedé, A. Chisvert, A. Salvador, D. Sánchez-Quiles, A. Tovar-Sánchez, Determination of UV filters in both soluble and particulate fractions of seawaters by dispersive liquid–liquid microextraction followed by gas chromatography–mass spectrometry, Anal. Chim. Acta 812 (2014) 50–58.

[33] M. Vila, J.P. Lamas, C. Garcia-Jares, T. Dagnac, M. Llompart, Ultrasound-assisted emulsification microextraction followed by gas chromatography–mass spectrometry and gas chromatography–tandem mass spectrometry for the analysis of UV filters in water, Microchem. J. 124 (2016) 530–539.

[34] J. López-Darias, V. Pino, J.L. Anderson, C.M. Graham, A.M. Afonso, Determination of water pollutants by direct-immersion solid-phase microextraction using polymeric ionic liquid coatings, J. Chromatogr. A 1217 (2010) 1236–1243.

[35] M. Schlumpf, B. Cotton, M. Conscience, V. Haller, B. Steinmann, W. Lichtensteiger, *In vitro* and *in vivo* estrogenicity of UV screens, Environ. Health Perspect. 109 (2001) 239–244.

[36] C. Schmutzler, I. Hamann, P.J. Hofmann, G. Kovacs, L. Stemmler, B. Mentrup, L. Schomburg, P. Ambrugger, A. Grüters, D. Seidlova-Wuttke, H. Jarry, W. Wuttke, J. Köhrlea, Endocrine active compounds affect thyrotropin and thyroid hormone levels in serum as well as endpoints of thyroid hormone action in liver, heart and kidney, Toxicology 205 (2004) 95–102.